Efficiency and stray light measurements and calculations of diffraction gratings for the Advanced Light Source

Wayne R. McKinney and Dmitri Mossessian
Accelerator and Fusion Research Division, Advanced Light Source, Lawrence Berkeley Laboratory, Berkeley, California 94720

Eric Gullikson
Materials Sciences Division, Center for X-ray Optics, Lawrence Berkeley Laboratory, Berkeley, California 94720

Philip Heimann
Accelerator and Fusion Research Division, Advanced Light Source, Lawrence Berkeley Laboratory, Berkeley, California 94720

(Presented on 21 July 1994)

Water-cooled gratings manufactured for spherical grating monochromators of the Advanced Light Source beamlines 7.0, 8.0, and 9.0 were measured with the laser plasma source and reflectometer in the Center for X-ray Optics at Lawrence Berkeley Laboratory. The square-wave gratings are ion milled into the polished electroless nickel surface after patterning by holographic photolithography. Absolute efficiency data are compared with exact electromagnetic theory calculation. Interorder stray light and groove depths can be estimated from the measurements. © *1995 American Institute of Physics.*

I. INTRODUCTION

We have previously reported on the collaboration which was formed to manufacture water-cooled gratings for synchrotron radiation.[1] Briefly, several laboratories and industrial companies joined together to make up a new source for holographically patterned, ion-milled square-wave profile gratings. All but two of these gratings have been delivered and all that have been installed at the Advanced Light Source (ALS) are functioning as designed in spherical grating monochromators. This paper reports the laboratory measurements performed on these gratings before installation.

The grating efficiency and stray light were evaluated using the laser plasma source and test tank in the Center for X-ray Optics at Lawrence Berkeley Laboratory (LBL).[2] This allows the testing of the gratings in the region from 40 to 500 Å in wavelength. The apparatus is diagrammed in Fig. 1. A frequency-doubled Nd:Y laser produces a plasma from a gold target. The compact monochromator has high acceptance with moderate resolution ($\lambda/\Delta\lambda \sim 300$). Two detectors of three different possible types generate the diffracted intensity and reference signals. All of the following motions are implemented: rotation of the sample, rotation of the detector, and *XYZ* translation of the sample.

II. GROOVE DEPTH MEASUREMENTS

Both for future reference and for the evaluation of the performance of the gratings in the various beamlines, it is necessary to know how closely the specified depth of the square waves was milled by the manufacturer into the electroless nickel substrate. The optimum groove depth was specified by using the exact differential method of grating efficiency calculation.[3] We found that while the efficiency curves predicted from the differential method were in general different from those generated by the simple scalar theory, the optimum groove depth selection was not affected by the choice of which theory was used. The actual groove depth was measured by varying the wavelength selected by the premonochromator with the grating under test and the detector fixed onto the zero order. The efficiency minimum corresponds to a $\lambda/2$ path length difference between the top and the bottom of the grooves. This concept is diagrammed in the scalar approximation in Fig. 2, and a typical data scan is shown in Fig. 3. Measurements become difficult below 100 Å depth, and the measurement of 55 Å listed below for the beamline 8.0 grating is near the limit possible for that grating with the wavelengths available.

Table I lists the specified and measured groove frequencies calculated and measured by these two methods. The measured depth data average 8% low with respect to the specified values. This may have resulted from the use of sputtered nickel on silicon wafers to calibrate the ion-milling procedure, or the use of the scalar model to infer the depths from the x-ray data. A small difference in etch rate between the sputtered and electroless types of nickel coating could explain this difference. In addition, the milling step must allow for the differential etch rates between the nickel, the

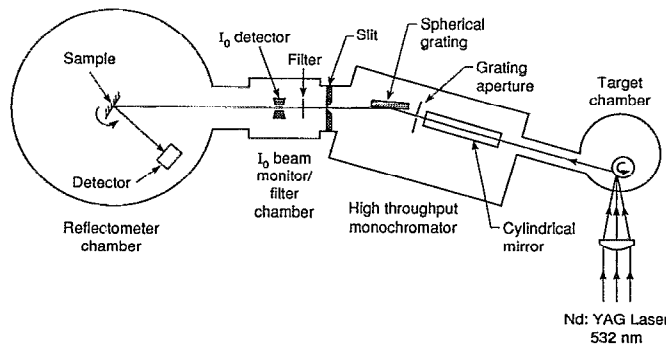

FIG. 1. Schematic diagram of the laser plasma source, premonochromator, and reflectometer in the Center for X-ray Optics.

 0034-6748/95/66(2)/2160/4/$6.00

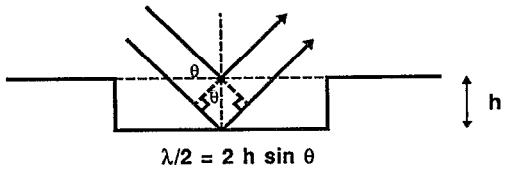

FIG. 2. Scalar theory diagram for interpretation of the minimum in zero-order efficiency for use in computation of the groove depth.

photoresist, and the components of an antireflection layer used in the process. The etch depths achieved were within the goal of ±10%, and were controlled sufficiently to provide good grating efficiency. Also, the zero-order measurement only sampled an approximately 1 mm sagittal band stretched out along the tangential direction on the grating, and did not test the entire surface. The fact that all of the measured depths are low suggests that the systematic difference, whether in the ion milling or in the measurement, can be eliminated in future gratings.

III. EFFICIENCY UNIFORMITY

The efficiency uniformity was measured during manufacturing by scanning an HeNe laser beam over the surface of the grating pattern at various steps in the process.[4] Figure 4 shows five parallel scans which covered the entire surface of the completed 380 mm beamline 9.0 grating. The beam was incident at 15° from normal. The uniformity is seen to be quite good in the visible, with a deviation of ±5%. The biggest deviation seen by this method on any grating was ±10%.

Four gratings were measured for uniformity in the soft x-ray region at various wavelengths from 100 to 200 Å. Because of the size of the water cooled gratings, the gratings could only be scanned a distance of 25 mm while the beam and geometry were held constant. These results are summarized in Table II. The values are consistent with the variation seen in the visible.

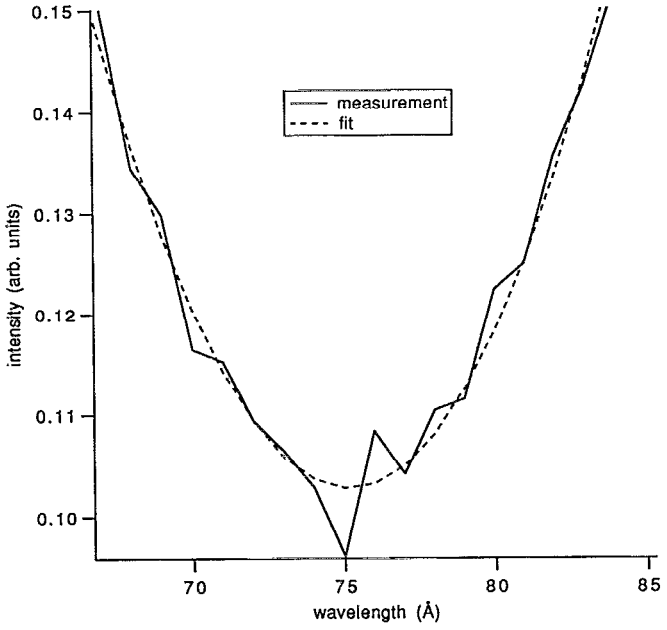

FIG. 3. Typical measurement of groove depth of by scanning the wavelength with the premonochromator while observing the zero order light.

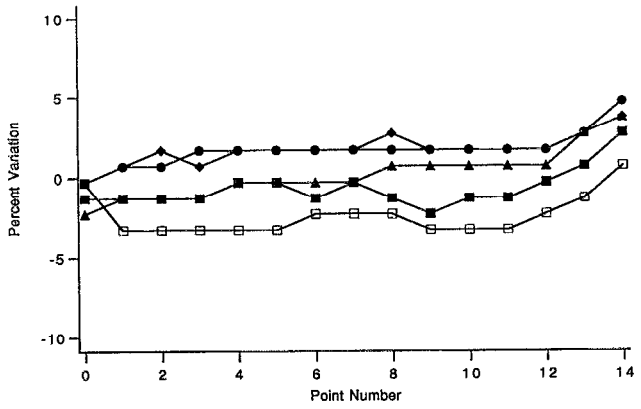

FIG. 4. Variation of grating efficiency across the whole surface of a grating in HeNe laser light at 15° incidence.

IV. INTERORDER STRAY LIGHT

As a measure of the stray light, we adopt the ratio of the average signal between the zero and first orders and the first-order intensity at its peak. This gives an upper bound on the stray light, as the stray light from the premonochromator is not characterized. Table III summarizes the gratings for which unambiguous measurements were taken. The nature of the electronics was such that small count rates were discriminated against when the zero order was on scale. The worst case of 26% stray light is the first grating which was cycled the most times during the fine tuning of the process. Repeatedly, processing the blank, that is, cleaning, exposing, developing, measuring, and stripping can cause some deterioration of the blank before the ion-milling process. In addition, the microroughness and chemical properties of the antireflection coating applied over the nickel can markedly affect the final grating performance. Differences in wettability were observed between the individual grating blanks.

A typical stray light scan is given in Fig. 5. Two conclusions are immediate. The stray light is a small fraction of the first-order signal, and the second order is also quite small.

TABLE I. Specified and measured groove depths.

Grating	Grooves per mm	Specified depth	Measured depth
Beamline 9.0	925	175 Å	161 Å
Beamline 9.0	380	350 Å	326 Å
Beamline 9.0	2100	90 Å	79 Å
Beamline 8.0	925	60 Å	55 Å
Beamline 8.0	380	130 Å	123 Å
Beamline 7.0	925	60 Å	not measured
Beamline 7.0	380	130 Å	120 Å
Beamline 9.3.2	1200	50	in progress

TABLE II. Uniformity of efficiency in the soft x-ray region.

Grating	Frequency	Length of scan	Variation
Beamline 8.0	925/mm	25 mm	±3.0%
Beamline 7.0	380/mm	25 mm	±4.0%
Beamline 9.0	380/mm	25 mm	±1.6%
Beamline 9.0	925/mm	25 mm	±1.4%

Typically, as shown in the figure, the second diffracted order was an order of magnitude smaller than the first order. This confirms the choice of the ALS of the square-wave profile for all of its initial complement of diffraction gratings.

V. ABSOLUTE EFFICIENCY

In addition to the depth of the pattern, the efficiency of square-wave gratings is also determined by the ratio of the width of the bottom to the width of the top of the grooves. The initial goal for this ratio was 0.5. Even though this ratio may to some advantage in efficiency be made as high as 0.7 to compensate for shadowing of the groove bottoms, the collaboration wished to limit the accumulated risk from attempting too much. The targeted value was changed to 0.55 as the project proceeded. This gave some assurance that even if the process latitude permitted a 0.05 error, the final grating would be at least half open grooves.

Figure 6 shows the experimental measurements and calculations for our most studied grating in terms of absolute efficiency. The open points are measured and the solid points are calculated. The experimental points have been removed to allow the four incidence angles used for the calculated points to be seen clearly. The measured depth of 123 Å was used with a 0.5 groove ratio. The calculation was done once with no fitting of parameters. The transverse magnetic (TM) and transverse electric (TE) efficiencies were averaged to allow for the essentially unpolarized plasma source. Each TM point was approximately 700 s compute time on a IBM RISC 6000 computer. The agreement is fairly good except for the minimum in the zero order. If more theoretical points were calculated, the curve would likely approach close to the minimum in the experimental curve, but at a different wavelength. The fact that scanning the angle instead of the wavelength indicates a different value for the depth of the grooves bears future investigation. The I/I_0 correction for the zero order can be affected by scattered light from the premonochromator.

TABLE III. Stray light measurements.

Beamline	Grooves	Wavelength	Stray light	Deg. Incident
BL 8.0	925/mm	100 Å	26%	10°
BL 7.0	925/mm	130 Å	10.2%	10°
BL 7.0	925/mm	130 Å	5.9%	5°
BL 7.0	925/mm	100 Å	11.1%	10°
BL 7.0	380/mm	130 Å	3.3%	5°
BL 7.0	380/mm	65 Å	14.1%	4.1°
BL 9.0	925/mm	130 Å	14.3%	5°
BL 9.0	925/mm	90 Å	4.9%	5.7°

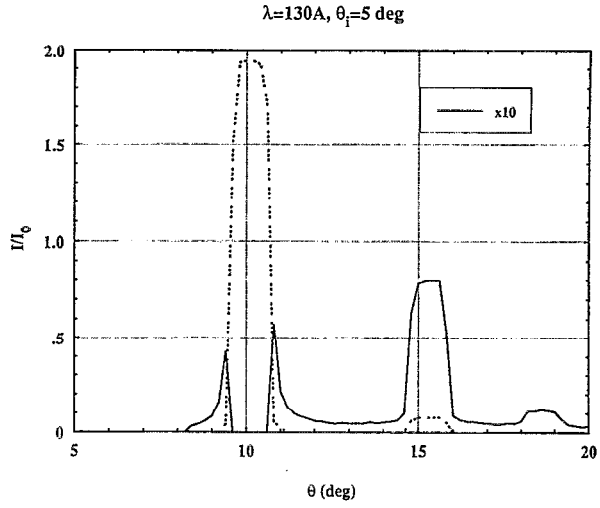

FIG. 5. Detector scan showing the zero, first, and second orders, used to determine interorder stray light. The solid line shows the same data as the dotted line multiplied by a factor of 10 to better show the interorder amplitude

VI. RESOLVING POWER

The resolving power of the gratings has been demonstrated in beamline 7.0 by the use of the N_2 absorption resonance at approximately 400 eV.[5] The measurement sets a lower limit on the resolving power of 8000, depending on the assumptions made for the widths of the peaks in the resonance. This completes the characterization of the gratings and is the consequence of the considerable time and expense dedicated to optical metrology and industrial collaboration.[6–8]

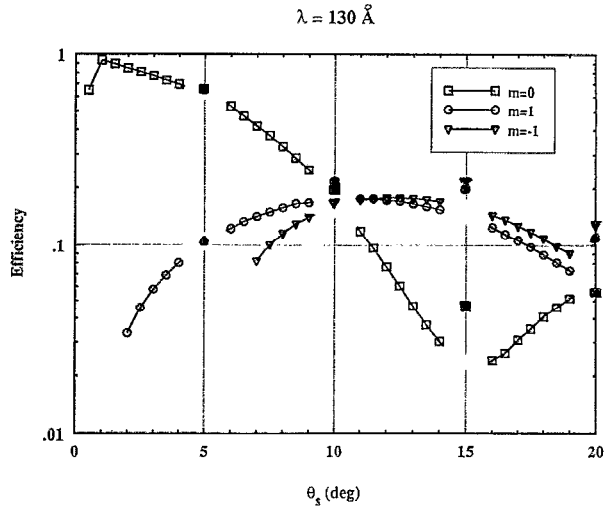

FIG. 6. Experimental absolute efficiency data (open marks), and theoretical calculation (closed marks). The x axis is plotted with the grazing angle of incidence rather than the angle measured from the normal.

VII. CONCLUSION

In summary, we find that the collaboration of Lawrence Berkeley Laboratory, and Argonne National Laboratory with industry (Photon Sciences, prime contractor, Rocketdyne Corp., Acteron Corp., and Hughes Aircraft, subcontractors) has provided a reliable source for state-of-the-art water-cooled, ion-milled square wave gratings for synchrotron beamline applications with good uniformity, efficiency, stray light, and resolving power.

ACKNOWLEDGMENTS

We wish to thank Clay Shannon and Earl Shults for the data on grating uniformity. We also thank Ben Wheeler for the calculation of grating efficiencies for Fig. 6, and Tica Valdes and Chris Palmer for the development of the vector grating efficiency program. This work was supported by the Director, Office of Energy Research, Office of Basic Energy Sciences, Materials Sciences Division of the U. S. Department of Energy, under Contract No. DE-AC03-76SF00098.

[1] W. R. McKinney, C. I. Shannon, and E. Shults, Nucl. Instrum. Methods Phys. Res. **347**, 220 (1993).
[2] E. M. Gullikson, J. H. Underwood, P. C. Batson, and V. Nitikin, J. X-Ray Sci. Technol. **3**, 283 (1992).
[3] V. Valdes, W. R. McKinney, and C. Palmer, Nucl. Instrum. Methods Phys. Res. **347**, 216 (1993).
[4] C. Shannon and E. Shults (private communication).
[5] T. Warwick, P. Heimann, D. Mossessian, W. McKinney, and H. Padmore, Rev. Sci. Instrum. (these proceedings).
[6] W. R. McKinney, S. C. Irick, and D. L. J. Lunt, Nucl. Instrum. Methods Phys. Res. A **319**, 179 (1992).
[7] W. R. McKinney, S. C. Irick, and D. L. J. Lunt, SPIE Proc. **1740**, 154 (1992).
[8] D. L. Lunt, J. W. Bender, D. G. Ewing, and W. R. McKinney, SPIE Proc. **1740**, 161 (1992).